Enhanced quadrupole collectivity at $N = 40$: The case of neutron-rich Fe isotopes

W. Rother,[1] A. Dewald,[1] H. Iwasaki,[2,3] S. M. Lenzi,[4] K. Starosta,[5] D. Bazin,[2] T. Baugher,[2,3] B. A. Brown,[2,3] H. L. Crawford,[2,6] C. Fransen,[1] A. Gade,[2,3] T. N. Ginter,[2] T. Glasmacher,[2,3] G. F. Grinyer,[2] M. Hackstein,[1] G. Ilie,[7,8] J. Jolie,[1] S. McDaniel,[2,3] D. Miller,[9] P. Petkov,[1,10] Th. Pissulla,[1] A. Ratkiewicz,[2,3] C. A. Ur,[4] P. Voss,[2,3] K. A. Walsh,[2,3] D. Weisshaar,[2] and K.-O. Zell[1]

[1]Institut für Kernphysik der Universität zu Köln, D-50937 Köln, Germany

[2]National Superconducting Cyclotron Laboratory, Michigan State University, East Lansing, Michigan 48824, USA

[3]Department of Physics and Astronomy, Michigan State University, East Lansing, Michigan 48824, USA

[4]Dipartimento di Fisica dell'Università and INFN, Sezione di Padova, I-35131 Padova, Italy

[5]Department of Chemistry, Simon Fraser University, Burnaby BC V5A 1S6, Canada

[6]Department of Chemistry, Michigan State University, East Lansing, Michigan 48824, USA

[7]Wright Nuclear Structure Laboratory, Yale University, New Haven, Connecticut 06520, USA

[8]National Institute of Physics and Nuclear Engineering, 76900 Bucharest, Romania

[9]Department of Physics and Astronomy, University of Tennessee, Knoxville, TN 37996, USA

[10]Institute for Nuclear Research and Nuclear Energy, Bulgarian Academy of Sciences, 1784 Sofia, Bulgaria

Abstract

The transition rates for the 2_1^+ states in ^{62,64,66}Fe were studied using the Recoil Distance Doppler-Shift technique applied to projectile Coulomb excitation reactions. The deduced E2 strengths illustrate the enhanced collectivity of the neutron-rich Fe isotopes up to $N = 40$. The results are interpreted using the generalized concept of valence proton symmetry which describes the evolution of nuclear structure around $N = 40$ as governed by the number of valence protons with respect to $Z \approx 30$. The trend of collectivity suggested by the experimental data is described by state-of-the-art shell-model calculations with a new effective interaction developed for the $fpgd$ valence space.

Configuration mixing is one of the most important concepts of quantum mechanics. Orbital mixing of electron configurations in organic molecules provides extra stability to the system; quark mixing accounts for rare meson decays violating the CP symmetry.

Configuration mixing in nuclear states provides a rich aspect of atomic nuclei, since it can considerably enhance amplitudes of collective excitation modes. Quadrupole deformation in nuclei is one such example and is known to evolve dramatically. Pronounced collectivity or deformation is normally observed in nuclei away from closed shells. It can be correlated with the dimension of the valence space, which is the product of valence proton and neutron numbers. This highlights a unique feature of atomic nuclei as a two fermionic quantum system.

Accumulated evidence has shown that magic numbers of nuclei can change far from the β stability line [1, 2]. This has challenged our familiar picture of the shell closure, motivating the quest to understand the evolution of collectivity and mixing properties of associated configurations at extreme isospin.

In the present work, we measured the mean lifetime (τ) of the first 2^+ (2^+_1) states of the neutron-rich ^{62,64,66}Fe isotopes at and around the neutron number $N = 40$. As a direct measure of quadrupole collectivity, we deduced the reduced E2 transition probabilities $B(\mathrm{E2};2^+\to0^+)$, which are inversely proportional to τ. Fe isotopes, spanning from the most neutron-deficient two-proton emitter $^{45}\mathrm{Fe}_{19}$ [3], via the most abundant isotope $^{56}\mathrm{Fe}_{30}$, to the most neutron-rich $^{74}\mathrm{Fe}_{48}$ hitherto observed [4], provide an intriguing testing ground for theoretical models to comprehend the evolution of collectivity over a wide range of neutron numbers. The $B(\mathrm{E2})$ values should follow an inverted parabola when plotted as a function of the neutron number going from the closed shell at $N = 20$ towards the next closed shell at $N = 28$ and then again from $N = 28$ to $N = 50$. The magicity at $N = 50$ is still an open question in the regime of large neutron excess. A key issue is the degree of collectivity manifested in $^{66}\mathrm{Fe}_{40}$ at the $N = 40$ harmonic-oscillator shell closure. If the $N = 40$ shell closure is absent – as suggested by the low excitation energy $E(2^+)$ of the 2^+_1 state in ^{66}Fe [5] – one can expect the maximum collectivity at $N \approx 40$, which corresponds to the middle of the magic numbers 28 and 50. In fact, a recent study indicated a sudden increase of $B(\mathrm{E2})$ from $^{62}\mathrm{Fe}_{36}$ to $^{64}\mathrm{Fe}_{38}$ [6]. However, this picture is in contrast to a doubly magic character of the neighboring $N = 40$ isotone $^{68}\mathrm{Ni}_{40}$, where a steep decrease of $B(\mathrm{E2})$ has been observed from ^{66}Ni to ^{68}Ni [7].

In this Letter, we investigate the interplay between quadrupole collectivity in ^{62,64,66}Fe and the configuration mixing of valence nucleons in terms of the semi-empirical scheme of the valence proton symmetry [8, 9] as well as state-of-the-art shell-model calculations. Based on new ^{66}Fe data and additional ones that are more precise than those given in [6], we provide a new insight into the complex evolution of collectivity in the vicinity of $N = 40$.

The experiment was performed at National Superconducting Cyclotron Laboratory (NSCL), Michigan State University. The lifetimes of the 2_1^+ states in ^{62,64,66}Fe were measured by means of the Recoil Distance Doppler Shift (RDDS) technique applied to intermediate-energy Coulomb excitation. This technique has been demonstrated for medium-heavy nuclei with proton number $Z \approx 50$ [9, 10]. We extended the RDDS measurements to lighter Fe projectiles with $Z = 26$ by optimizing the target-degrader combination of the Köln/NSCL plunger device [9–11]. By making use of intense secondary beams provided by the Coupled Cyclotron Facility at NSCL, the Segmented Germanium Array (SeGA) for gamma-ray detection, and the S800 spectrograph [12] for identification of reaction products, we realized the lifetime measurements of neutron-rich Fe isotopes up to $N = 40$.

Secondary beams of Fe were produced by fragmentation of a primary ^{76}Ge beam at 130 AMeV incident on ^{9}Be targets. The A1900 fragment separator [13] was used to purify the fragments. The resulting beam was ≈85% ^{62}Fe (at a typical rate of 3.6×10^4 pps and an incident energy of 97.8 AMeV), ≈65% ^{64}Fe (6×10^3 pps, 95.0 AMeV), and ≈25% ^{66}Fe (1×10^3 pps, 88.3 AMeV) for each setting.

The beams were directed onto the plunger device, which was mounted at the target position of the S800 spectrograph. The plunger target was a 300 μm-thick Au foil, while a 300 μm (400 μm)-thick Nb foil was used as a degrader for the ^{62,66}Fe (^{64}Fe) measurement. The beam velocities before and after the degrader were estimated to be $v/c = 0.368$, 0.322 for ^{62}Fe, $v/c = 0.364$, 0.298 for ^{64}Fe, and $v/c = 0.346$, 0.291 for ^{66}Fe, respectively, with typical velocity widths (in r.m.s.) of ≈1%. Mass and charge of the incoming beams were identified event-by-event using the time-of-flight measured as the timing difference between two plastic scintillators placed in the extended focal plane of the A1900 and in the object plane of the S800 analysis beam line. Scattered particles were identified by the detection system of the S800 [12].

Doppler-shifted γ rays were detected by SeGA with the digital data acquisition system [14]. Two rings of 7 and 8 detectors were mounted at forward and backward angles of 30° and 140° relative to the beam axis. Data were taken at $5 - 7$ different target-degrader distances over the range from 0 to 20 mm for different Fe isotopes. The data taken at the largest distances were used to examine the contributions from reactions in the degrader [9, 11].

Lifetimes were determined by line-shape analysis in a similar procedure to those developed in Refs. [9, 11]. The best-fit results for each Fe isotope are shown in Fig. 1. The calculation takes into account the velocities of the incoming and outgoing beams, the energy losses through the target and degrader, and the detector geometry including effects due to the Lorentz boost. The energy and angular straggling of the reaction products and the energy resolution of the γ-ray detectors are described as a single width parameter of a Gaussian distribution incorporated in the lineshapes. We used four different width parameters for decays before and after the degrader in the spectra obtained with the forward and backward rings. The fits to the data were performed using variable parameters which include the lifetime of the state of interest, the width parameters, a normalization factor, as well as the yield ratio between target and degrader. The large distance data were found to be consistent with degrader-to-target yield ratios of around 30–40 % for ^{62,64,66}Fe.

In the present analysis, special care was taken to select sensitive regions of the spectra which ensure the reliability of our χ^2 analysis in determining the lifetime. To this end, after fixing the parameters that characterize the lineshape, we compared the simulated spectra to the measured ones by varying only the lifetimes. It became obvious that the most sensitive region corresponds to the γ-ray energy range closest to the two peak centroids. It is worth noting that the peak amplitudes are most sensitive to the lifetime, whereas the χ^2 value can also be affected by details of the lineshape. Therefore, we restricted the χ^2 calculation to the optimum regions as indicated by the data with the error bars in Fig. 1. We found a higher sensitivity to the lifetime for the spectra obtained from the forward-ring detectors. We thus first made a fit only to the forward-ring spectra to search for the χ^2 minimum over a wide range of the lifetime. Later, we determined the lifetime from an overall fit around the obtained minimum using the data taken with both rings. The results of τ are summarized in Table I, together with the corresponding $B(\mathrm{E2};2^+\rightarrow0^+)$ values. The final lifetime results are consistent with the first results obtained with the forward-ring data. For ^{62}Fe, we used only forward-ring data due to a contaminant in the backward-ring spectra.

The evolution of collectivity for even-even nuclei with $Z = 24 – 36$ and $N = 22 – 58$ is studied in Fig. 2 from the systematic behavior of the $E(2^+)$ (Fig. 2 (a)) and B(E2;$2^+ \rightarrow 0^+$) values (Fig. 2 (b)) [15–27]. Only Ni isotopes reveal characteristics of shell closure at $N = 28$, 40 as inferred from large $E(2^+)$ and small B(E2) values. The $N = 40$ shell closure vanishes for all the other even-even isotopes, where an enhanced collectivity is evident. The present B(E2) data confirm the onset of collectivity for ^{62,64}Fe recently reported [6] (see Table I) and represent the first evidence for the enhanced colletivity in ^{66}Fe at $N = 40$. The B(E2) of ^{64,66}Fe correspond to a large deformation parameter of $\beta_2 \approx 0.28$.

Interestingly, one can see in Fig. 2 (a) notable similarities in the $E(2^+)$ behavior for the pairs of Fe ($Z = 26$)/Se ($Z = 34$), and Zn ($Z = 30$)/Ge ($Z = 32$) [16]. An incipient similarity in $E(2^+)$ is also suggested for the Cr ($Z = 24$)/Kr ($Z = 36$) pair. The enhancement of collectivity is also noticeable from the decrease of $E(2^+)$ as one moves away from the proton number $Z \approx 30$. It starts at $N = 36$ for Cr/Kr, $N = 38$ for Fe/Se and $N = 40$ for Zn/Ge, respectively. These striking similarities suggest an isotonic symmetry in the development of collectivity for each of these pairs.

To further investigate the underlying symmetry inferred from the $E(2^+)$ behavior, we turn to the valence proton symmetry (VPS) [8, 9]. The VPS scheme correlates a pair of isotones that have the same number of valence proton holes and particles with respect to closed shells. The same valence space for correlated nuclei results in a similar degree of collectivity and its evolution, as shown, for example, in the region of $50 < N < 82$ and $Z \approx 50$ [9]. Here, we generalized the VPS concept since the symmetry appears with respect to $Z = 30$ instead of the magic number $Z = 28$. Namely, we consider proton holes in the $1f_{7/2}$ orbital below $Z = 28$ and protons in the $1f_{5/2}$ orbital above the $Z = 32$ subshell closure. This is justified by the fact that the $2p_{3/2}$ orbital is isolated between the $1f_{7/2}$ and $1f_{5/2}$ orbitals. The $2p_{3/2}$ orbital, if it is fully occupied, has no impact on the evolution of collectivity, and hence, for the VPS scheme, the effect of a fully empty or occupied $2p_{3/2}$ orbital is identical. Consequently, Se (Kr) can be a valence partner of Fe (Cr).

While the energies of valence partner nuclei can be compared directly and show a good agreement (Fig. 2 (a)), one has to apply a scaling factor to the B(E2) values by which charge and mass differences are considered in the comparison. For the heavier partners (Se and Kr), the scaling factor $S = (Z_L/Z_H)^2 \times (A_L/A_H)$, has to be used. Z_H and A_H (Z_L and A_L) denote the atomic and mass numbers of heavier (lighter) partners [9]. This is illustrated in Fig. 2 (c), where we compare the existing B(E2) data for the Fe/Se and Cr/Kr pairs including the present data of ^{62,64,66}Fe. For the B(E2) values of the Fe/Se pair, we find a good agreement at $N = 34$ and $N = 36$ and deviations at larger neutron numbers $N = 38$ and 40. The Fe value is above the scaled Se value at $N = 38$ and, for $N = 40$, below the scaled Se value. Taking into account the experimental errors, one can state that the Fe B(E2) values follow the trend of increasing collectivity from $N = 36$ towards $N = 40$ or 42 and scatter around the corresponding Se values. Perfect overall agreement cannot be expected. The VPS concept is only suited to describe gross features of nuclear structure since it is parameter free. Using the VPS for predicting collectivity for more neutron-rich nuclei, similar B(E2) values are expected for heavier Fe isotopes and corresponding Se isotopes at $N \geq 42$. This is consistent with the result of new state of the art shell-model calculations as shown below. The calculated B(E2) values for $N = 40$ and 42 agree almost perfectly (Fig. 2 (c)). For heavier Fe nuclei no shell-model results are available and so far only the VPS is available to give perspectives for the development of collectivity of Fe at extreme isospin.

For Cr nuclei the 2_1^+ energies also agree nicely with those of the Kr valence partners. The B(E2) values have been measured only up to $N = 34$ and, for Kr, down to $N = 36$. This means that a direct test of the VPS is not possible at the moment. It should be interesting to note that the shell-model calculations for Cr nuclei (in Fig. 2 (c) the result for $N = 36$ is given) agree perfectly with the scaled krypton B(E2) values from the VPS. The VPS concept provides gross predictions for highly neutron-rich nuclei, which will be examined by future experiments at new rare-isotope facilities under construction.

The observed isotonic symmetry points to similarities in the role played by protons in the $1f_{5/2}$ orbital and proton holes in the $1f_{7/2}$ orbital for the development of collectivity. In a shell-model picture, these orbitals play an important role in changing the neutron shell gap at $N = 40$ due to the proton-neutron monopole tensor interaction [27]. For Fe isotopes that have proton holes in the $1f_{7/2}$ orbital, the attractive interaction with the neutron $1f_{5/2}$ orbital and repulsive interaction with the $1g_{9/2}$ and $2d_{5/2}$ orbitals get weaker [27], reducing the $N = 40$ gap.

To allow a quantitative discussion of the intruder neutron configurations for the enhanced collectivity of neutron-rich Fe isotopes, we have performed shell-model calculations [28] and compare them with the present B(E2) data for ^{62,64,66}Fe. The natural choice for the model space is the fp shell ($20 \leq Z \leq 40$) for protons and the $2p_{3/2}1f_{5/2}2p_{1/2}1g_{9/2}$ space for neutrons ($28 \leq N \leq 50$). However, shell-model calculations in this model space fail to fit the ^{66}Fe 2_1^+

state [27], while they can reproduce the level schemes of $^{62-64}$Fe rather well. To reproduce the quadrupole collectivity in this mass region, the inclusion of the neutron $2d_{5/2}$ orbital is necessary [2].Recently, a new effective interaction for this large model space (LNPS) has been developed that can reproduce the different phenomena suggested by the available data in this mass region [28]. The results for the $E(2^+)$ and B(E2) values obtained with standard effective charges ($e_n = 0.5e, e_p = 1.5e$) for the Fe isotopes of interest are reported in Table I. The excitation energies agree very well with the calculations in all cases. The calculated B(E2) of ^{64}Fe coincides with the data. For ^{62,66}Fe, the experimental values are overestimated by about 20–30% that decrease considerably if the error bars are taken into account. The observed rapid increase of collectivity is well described by the shell-model. It should be noted that the present calculations do not intend to be a best fit but describe the evolution of collectivity in a vast region. The present data constitute valuable information to improve this description. The analysis of the calculated ground state wave functions shows that in ^{62}Fe, the probability of excitations to the upper gd orbitals is about 60%, increasing to $\sim$ 90% in ^{64}Fe and to almost 99% in ^{66}Fe, in agreement with the development of deformation approaching $N = 40$ shown by the data. This is consistent with the development of a new "island of inversion" at $N = 40$.

In summary, we measured the lifetimes of the 2_1^+ states of ^{62,64,66}Fe, quantifying for the first time an enhanced collectivity of the Fe isotopes at $N = 40$. The observed trends in $E(2^+)$ and B(E2) strongly support the isotonic symmetry with respect to the proton number $Z \approx 30$, suggesting that the region of enhanced collectivity extends to neutron-rich Fe and Cr isotopes beyond $N = 40$. The shell-model calculations with the new effective LNPS interaction account for the rapid development of deformation toward N=40 and describe the present B(E2) data fairly well. The calculations point to the important role of the neutron intruder configurations across the $N = 40$ subshell gap due to the shell migration far from stability.

The authors thank F. Nowacki, A. Poves and K. Sieja for fruitful discussions. This work is supported by the US NSF under PHY-0606007, PHY-0758099, and MRI PHY-0619497, and also partly by the DFG (Germany) under DE1516/1-1 and GSI, F.u.E. OK/JOL.

[1] T. Otsuka *et al.*, Phys. Rev. Lett. 104, 012501 (2010).

[2] E. Caurier *et al.*, Eur. Phys. J. A15, 145 (2002).

[3] J. Giovinazzo *et al.*, Phys. Rev. Lett. 89, 102501 (2002).

[4] T. Ohnishi *et al.*, J. Phys. Soc. Jpn. 79, 073201 (2010).

[5] M. Hannawald *et al.*, Phys. Rev. Lett. 82, 1391 (1999).

[6] J. Ljungvall *et al.*, Phys. Rev. C 81, 061301(R) (2010).

[7] O. Sorlin *et al.*, Phys. Rev. Lett. 88, 092501 (2002).

[8] R. F. Casten and N. V. Zamfir, Phys. Rev. Lett. 70, 402 (1993).

[9] A. Dewald *et al.*, Phys. Rev. C 78, 051302(R) (2008).

[10] A. Chester *et al.*, Nucl. Instrum. Meth. A 562, 230 (2006).

[11] K. Starosta *et al.*, Phys. Rev. Lett. 99, 042503 (2007).

[12] D. Bazin *et al.*, Nucl. Instrum. Meth. B 204, 629 (2003).

[13] D. J. Morrissey *et al.*, Nucl. Instrum. Meth. B 204, 90 (2003).

[14] K. Starosta *et al.*, Nucl. Instrum. Meth. A 610, 700 (2009).

[15] Evaluated Nuclear Structure Data File (ENSDF), http://www.nndc.bnl.gov/ensdf.

[16] N. Hoteling *et al.*, Phys. Rev. C. 74, 064313 (2006).

[17] N. Aoi *et al.*, Phys. Rev. Lett. 102, 012502 (2009).

[18] A. Gade *et al.*, Phys. Rev. C81, 051304(R) (2010).

[19] A. Bürger *et al.*, Phys. Lett. B 622, 29 (2005).

[20] P. Adrich *et al.*, Phys. Rev. C 77, 054306 (2008).

[21] E. Padilla-Rodal *et al.*, Phys. Rev. Lett. 94, 122501 (2005).

[22] T. Rzaca-Urban *et al.* , Eur. Phys. J. A9, 165 (2000).

[23] E.F. Jones *et al.*, Phys. Rev. C 73 017301 (2006).

[24] J. Ljungvall *et al.*, Phys. Rev. Lett. 100, 102502 (2008)

[25] A. Obertelli *et al.*, Phys. Rev. C 80, 031304(R) (2009)

[26] J. Van de Walle *et al.*, Phys. Rev. C 79, 014309 (2009).

[27] S. Lunardi *et al.*, Phys. Rev. C 76, 034303 (2007).

[28] S. M. Lenzi *et al.*, Phys. Rev. C82 , 054301, (2010).

Table I: Comparison between the experimental (Exp) and theoretical (SM: shell-model) $E(2^+)$ and $B(\mathrm{E2})$ values for ^{62,64,66}Fe. The lifetimes (τ_{Exp}) are the present results, while the $E(2^+)$ values are taken from Ref. [27]. Previous $B(\mathrm{E2})$ data (Pre) [6] are also compared.

A	τ_{Exp} [ps]	$E(2^+)$ [keV]		$B(\mathrm{E2})$ [$e^2\mathrm{fm}^4$]		
		Exp	SM	Exp	Pre	SM
^{62}Fe	8.0(10)	877	835	198(25)	214(26)	270
^{64}Fe	10.3(10)	746	747	344(33)	470^{+210}_{-110}	344
^{66}Fe	39.4(40)	575	570	332(34)		421

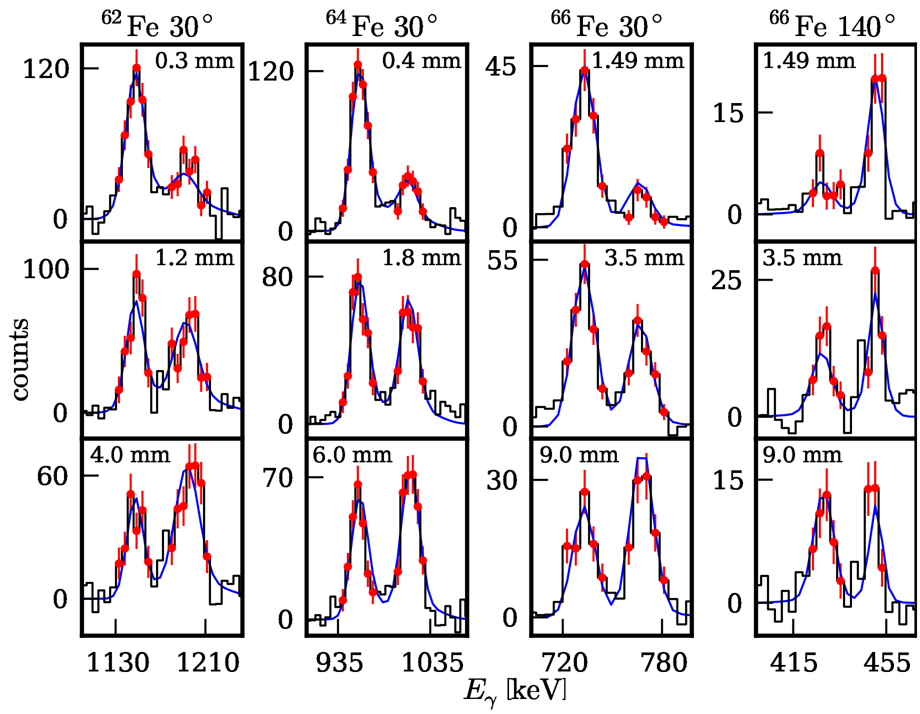

Figure 1: Typical results from the γ-ray line-shape fits to the data for the $2^+\to0^+$ transitions in ^{62,64,66}Fe.

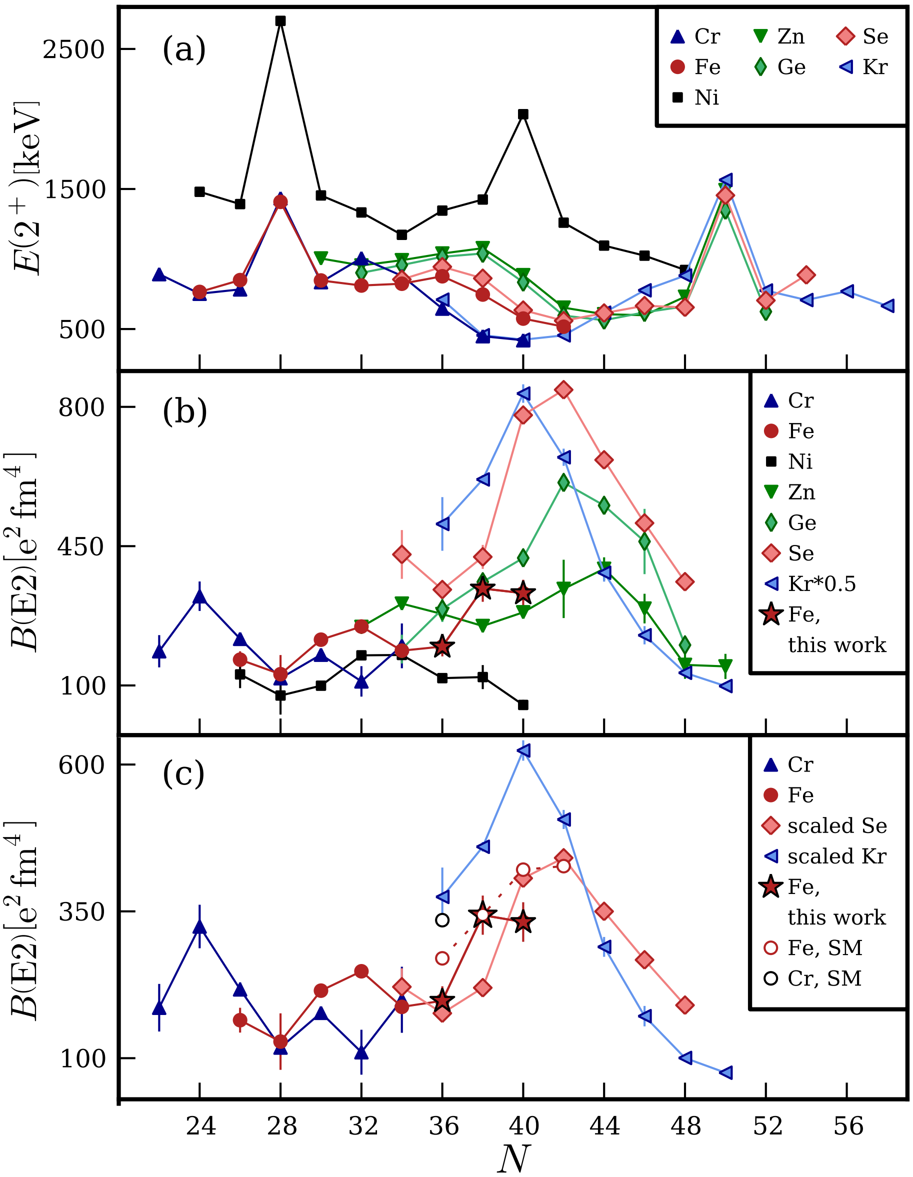

Figure 2: (a) Energies $E(2^+)$ and (b) $B(\mathrm{E2};2^+\!\rightarrow\!0^+)$ values for even-even nuclei with $Z = 24 - 36$ and $N = 22 - 58$. The stars indicate the present data of ^{62,64,66}Fe. The B(E2) data of Kr in (b) are divided by 2. In (c), the B(E2) data of the Fe and Cr isotopes are compared to the scaled B(E2) values for the Se and Kr isotopes, respectively, as well as the shell-model predictions (SM) for ^{62,64,66,68}Fe and ^{60}Cr isotopes.